Chapter 3

Expression of chronodisruptive miR34a-5p in atherosclerosis and its regulation by carbon monoxide releasing molecule-A1

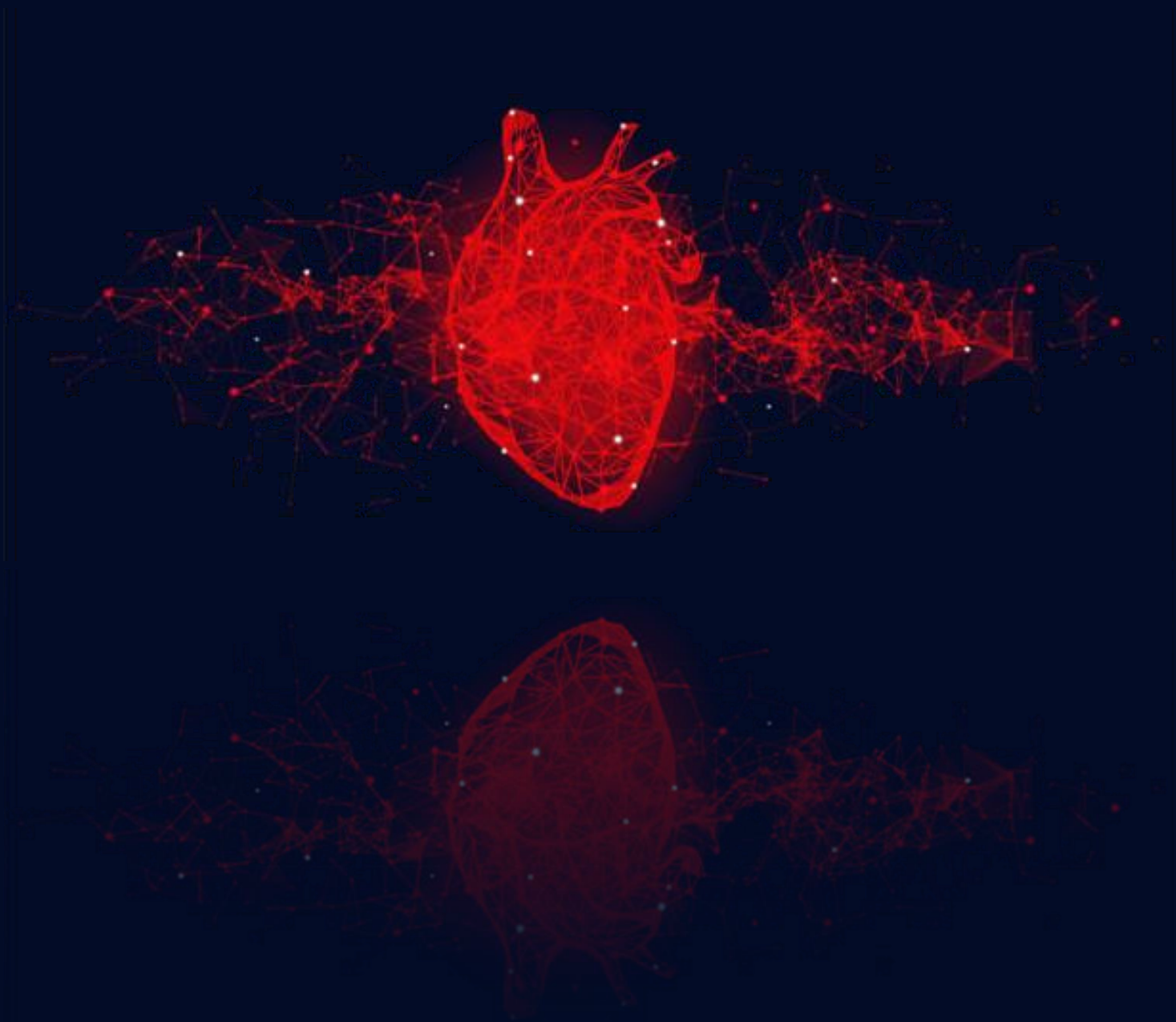

Introduction

Pertaining to current lifestyle and socio-environmental changes there has been a steep rise in plethora of cardiovascular disorders viz. ischemic heart disease, heart attacks, thrombosis and arteriosclerosis (Sharifi-Rad *et al.*, 2020). Atherosclerosis is marked by excessive lipid uptake culminating in endothelial dysfunction, foam cell formation and eventually into atheromatous plaque formation. It is a multifactorial disorder with chronodisruption as one of the key causative agents that has been widely studied over the decades. Chronodisruption predisposes biological system of an individual to atherosclerosis via persistent low-grade inflammation, ROS, cellular oxidative stress, lipid accumulation and mitochondrial dysfunction that acts as major pro-atherogenic changes (Wilking *et al.*, 2013; McAlpine and Swirski, 2016). There have been several attempts to ameliorate atherosclerosis primarily by symptomatic treatment and secondarily by inculcating a wholistic amendment in lifestyle including correct food and water intake, exercising and correcting sleep-wake cycles.

A plethora of cardiovascular drugs have been discovered and are sold over the counter. These drugs are symptom oriented and combat singular concern at a time viz. some of the well used statins are targeted towards lipid lowering and fail to address an inflammatory response, while others orchestrate pleotropic effects. Atherosclerosis is a multifaceted and a multi-stage disorder making it grim to develop a drug addressing the root cause of the said pathology. In an attempt to do so, new therapeutic strategies are being explored that focuses on utilising biomolecules to combat the pathophysiology in the most natural and effective ways. Past decade has witnessed and unveiled commendable potential of miRNAs as a key signalling and regulatory molecule involved in the initiation and progression of atherosclerosis. Studies have shown

circadian regulation of several miRNAs that also happen to have role in metabolic physiology. In previous chapter we have reported miR34a-5p to be playing functional role in circadian biology by regulating CLOCK gene expression.

miR34a has been reported to be widely functional in varied pathophysiological conditions including cancers, atherosclerosis, fatty liver, Non-alcoholic steatohepatitis etc. (Slabáková *et al.*, 2017; Li *et al.*, 2018b; Xu *et al.*, 2021). Microarray analysis of atheromatous plaque showed elevated levels of miR34a. The same was recorded in circulation of the CVD patient and is also proposed as potential biomarker for cardiovascular disorders (Han *et al.*, 2015). However, the regulatory axis of miR34a-5p remains unexplored in atherogenic pathologies. miR34a-5p is an intergenic miRNA and is transcribed with its own promoter region. miR34a-5p is in tight feedback loop control of its key transcription factor P53 (Shetty *et al.*, 2017). There are several other regulators that impact miR34a-5p transcription that are yet unexplored in atherogenic pathophysiology.

Carbon monoxide (CO) is by-product of rhythmic heme degradation and a vital gasotransmitter (Siracusa *et al.*, 2021). Physiologically CO is important in mediating cell-cell interaction and maintaining vasomotor tone for a healthy vasculature. Along with that CO is studied to have circadian regulatory control by inhibiting CLOCK – BMAL1 to binding to their target promoter (Klemz *et al.*, 2017). Moreover, systemic removal of CO leads to circadian clock disruption and impending neuronal cell-cell connection (Minegishi *et al.*, 2018). CO is also reported to have metabolic control by regulating several gene expression along with cellular redox status (Choi *et al.*, 2012). A cohort-based study had reported elevated CO levels in the patients with CVDs (Cheng *et al.*, 2010). Colloquially CO has received bad connotation as a toxin pertaining to the fact that exposure to excessive CO can be lethal, however delimited exogenous CO has

therapeutic potential. CO has been implicated in regulating mitochondrial ROS, cytochrome c oxidase, oxygen consumption, oxidative metabolism, and overall mitochondrial functioning. Carbon monoxide releasing molecule A1 (CORM A1) is an organometallic compound with a boron core that facilitates slow and controlled release of CO (Motterlini *et al.*, 2005). The therapeutic efficacy of CORM-A1 is well established in several disease models including diabetes, myocardial infarction, and posterior uveitis.

This study is the compile of investigating miR34a-5p regulation in atherogenic pathophysiology using in-vivo (atherogenic diet fed Sprague Dawley Rats) and in-vitro (ox-LDL treated HUVEC and Monocyte Derived Macrophages; MDMs) experimental models. Further, mechanism of circadian clock associated miR34a-5p expression/production in atherogenic milieu is investigated along with using CORM-A1 as a modulator. The study aims at addressing status of chronodisruptive miR34a-5p in pro-atherogenic milieu and its alterations by chrono-metabolic controller CO.

Methodology

In-vivo Experimentations

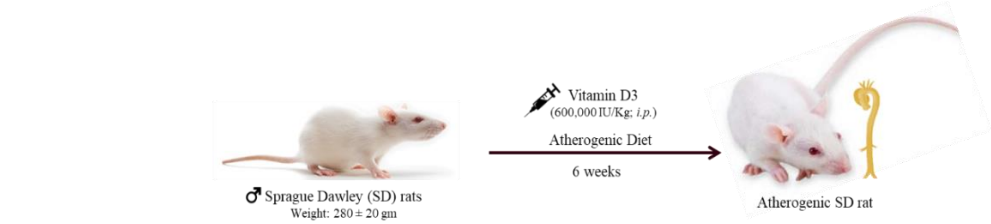

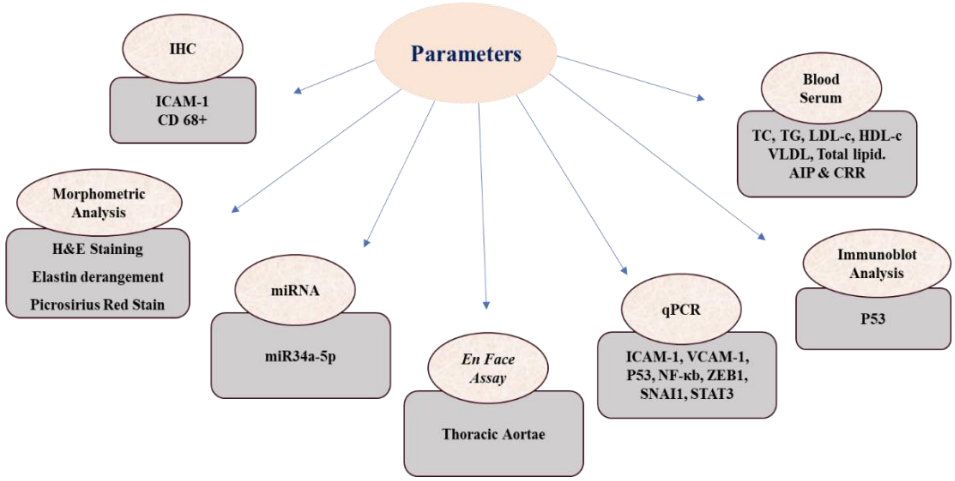

In-vitro Experimentations (HUVEC)

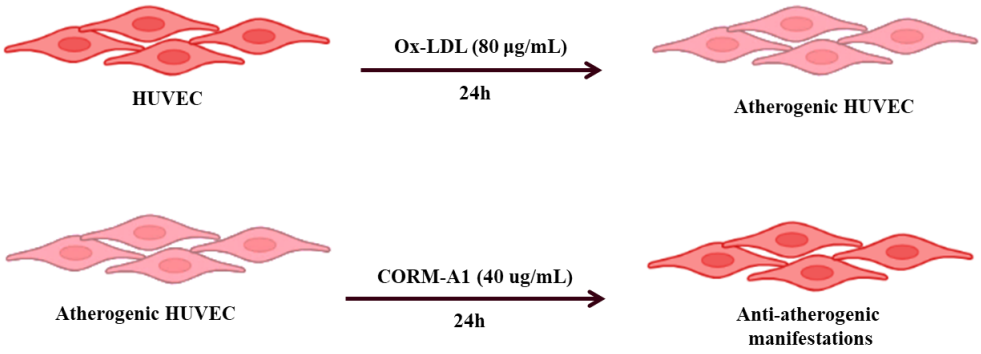

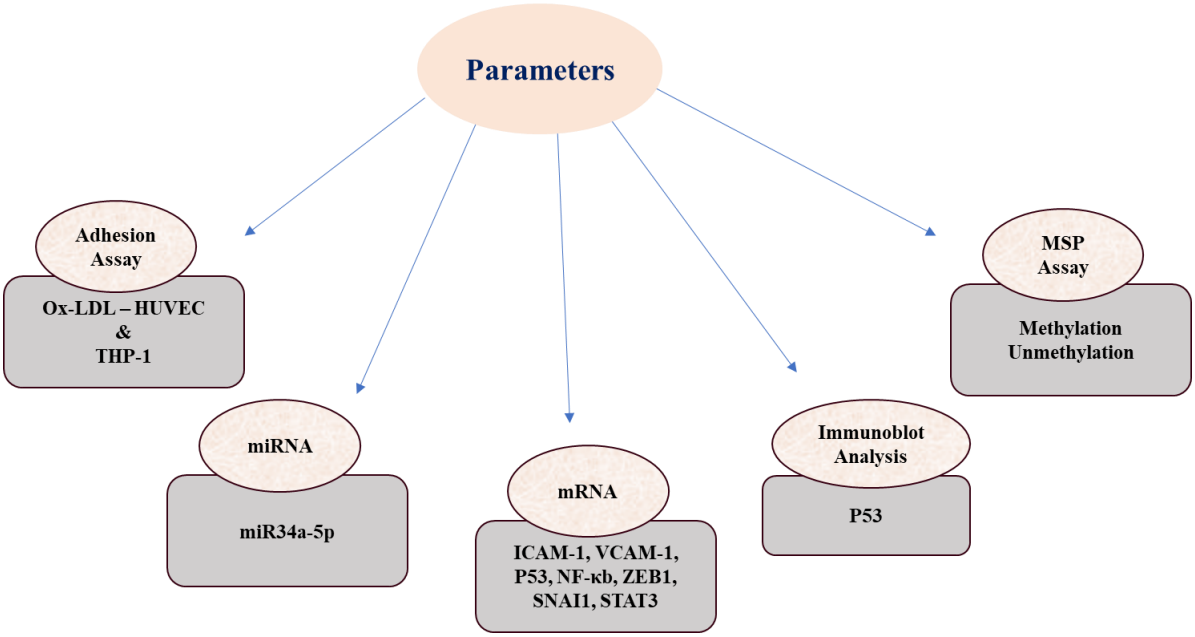

In-vitro Experimentations (MDMs)

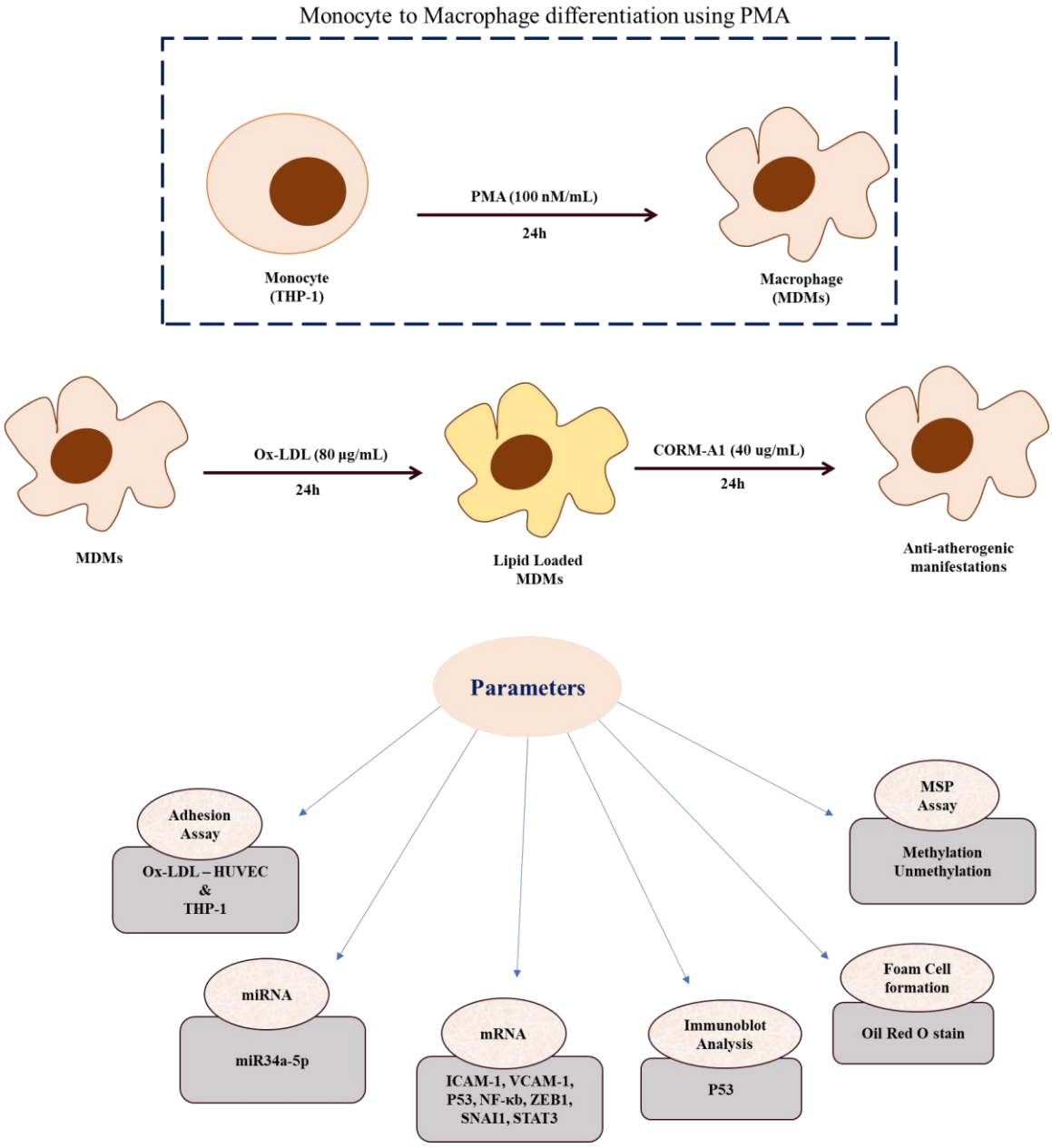

Results

Deciphering circadian association of Carbon monoxide

Circadian rhythm of the body is fine-tuned with interplay of several biomolecules. Carbon monoxide have been reported for its chronobiological control in several studies. Herein we validated the same using CytoScape V 3.8.2 database to generate the circadian implications of carbon monoxide studies in human physiology. Data showed that the by-product of rhythmic heme degradation, CO regulates CRY1, CRY2, PER1, PER2, TIMELESs and NR1D1 genes (Fig 3.1). This was in agreement with the published literature that shows CO mediated impending of CLOCK – BMAL1 heterodimer binding to the transcription start site of period and cryptochrome family genes. Overall suggesting CO functioning as a circadian clock modulator.

CORM-A1 ameliorates pro-atherogenic manifestations in atherogenic diet fed SD rats

Diet induced alteration leading to CVDs, pertaining to current lifestyle, was tried to attain by feeding atherogenic diet to SD rats. Aortae of ath diet fed SD rats showed proatherogenic manifestations that were reverted in the CORM-A1 treated group. Physiological evaluations with *En face* assay exhibited arterial stiffening and lesions in ath diet fed SD rats, wherein CORM-A1 treated animals showed no trace of arterial lesions (Fig 3.2). The histomorphological evaluations in H&E-stained section of thoracic aorta reveled vascular derangement and enhanced intimal-media thickness that was significantly restored on CORM-A1 treatment (Fig 3.3.1a). Further enhanced elastin derangement and fragmentation was also restored on CORM-A1 treatment (Fig 3.3.1b). Collagen content of aorta increases in atherogenic conditions resulting into

arterial stiffening and obstructed vasomotor tone. The same was evaluated in the thoracic aortae of SD rats by Picrosirius Red staining. Aortae of ath diet fed SD rats had exhibited higher collagen content as compared to that of the control and ath + CORM-A1 administered rats (Fig 3.3.1c). Further, collagen/elastin ratio was also improved in CORM-A1 co-supplemented animals, displayed improvement in vasomotor tone. No difference was observed in ath diet fed SD rats administered with iCORM-A1 (Fig 3.3.2) and hence the same was not taken further in other experimentations.

Serum lipid Profiling of atherogenic and CORM-A1 treated SD rats

Serum lipid profile was assessed for all the animals. Wherein ath diet fed SD rats had shown higher titers of total serum cholesterol, VLDL, LDL, triglycerides, and total circulating lipid content along with significantly lowered HDL levels. The LDL/HDL and Chlo/HDL ratios were also higher in ath group. Whereas the CORM-A1 treated animals showed corrective changes with reduction in the ratios and lowering titers of VLDL, total cholesterol, lipid, LDL and triglycerides (Fig 3.4a). The same were used to calculate Atherogenic Index of Plasma (AIP) and Cardiac Risk Ratio (CRR) that were elevated in ath diet fed SD rat and exhibited significant reduction in CORM-A1 group (Fig 3.4b).

Cytotoxicity of CORM-A1 in HUVEC and MDMs

HUVECs and THP-1 derived MDMs (procedure mentioned in material and methodology section) were treated with different doses (10, 30, 40, 50, 100 & 200 μM) of CORM-A1 for 24 h and cell viability was assessed by MTT assay. A non-significant

change in cell viability was observed in lower doses of 10, 30 & 40 μM, whereas the higher doses of 50, 100 & 200 μM exhibited more than ~80% cell viability in HUVEC (Fig. 3.5a). On contrary non-significant changes in cell viability were observed at all the doses in MDMs (Fig 3.5b).

CORM-A1 impedes miR34a-5p in normal physiological conditions in HUVEC and MDMs

Chapter 1 and 2 talked about circadian association and control of miR34a-5p in the physiological conditions with an indication of plausible implications in atherogenic pathology. Herein, we assessed if there is a direct impact of CO on expression of miR34a-5p. HUVECs and THP-1 derived MDMs were treated with 40 and 100 μM of CORM-A1 for 24h. miR34a-5p expression when normalized to 5S showed significantly ($P < 0.05$) lowered expression in 40 μM dose as compared to the control, whereas 100 μM treated cells showed about 4 times upregulation. The established target of miR34a-5p, SIRT-1 was further quantified for the same doses to find antagonistic expressional response in both the cell types, as anticipated (Fig 3.6). Cumulatively, CORM-A1 exhibited dose dependent response on expression of miR34a-5p in both the cell types, unveiling the miRNA modulatory capacity in normal cellular physiology. Thus, 40 μM of CORM-A1 was used further for all the experimentations.

CORM-A1 ameliorates atherogenic changes in HUVEC and MDMs

Endothelial dysfunction and foam cell formation marks the initiation of proatherogenic changes in the artery. To assess the anti-atherogenic potential of CORM-A1 in an invitro

system HUVEC and MDMs were treated with ox-LDL (80 µg/mL) and/or CORM-A1 (40 µg/mL). Atherogenic changes in HUVEC were assessed by expression analysis of adhesion molecules (*Icam-1* and *Vcam-1*) that are elevated in atherogenic conditions. Ox-LDL treated cells showed elevated expression of these adhesion molecule as anticipated, whereas CORM-A1 co- treatment had resulted into lowered expression of these molecules, in agreement to the results obtained in adhesion assay (Fig 3.7a).

Atherogenic manifestations in macrophages are normally depicted with foam cell formation resulting of all the accumulated lipid content in the cells. ox-LDL treated MDMs showed prominent lipid uptake and foam cell formation, as evidenced by ORO staining, the same was observed to be reverted in CORM-A1 co-treated cells (Fig 3.7b). Cumulatively, CORM-A1 exhibits anti-atherogenic potential even in in-vitro experimental models.

CORM-A1 alleviates miR34a-5p by altering expression of its transcription factors

Patients with atherosclerosis are studied to have elevated miR34a-5p titers in atheromatous plaque. Herein, we observed results in agreement to the patient study in the thoracic aortae of ath diet fed SD rats as well as ox-LDL treated HUVEC and MDMs (Fig 3.8a). However, there exist a lacuna pertaining to miR34a-5p production in pathogenic conditions. To investigate the same, we assessed transcription factors of miR34a-5p, P53 and NF-κB in thoracic aortae along with HUVEC and MDMs. Moreover, an attempt to assess the mechanism of CORM-A1 mediated lowering of miR34a-5p was also made herein. Levels of *P53* had shown elevation in thoracic aortae of ath diet SD rats, however no significant change was observed in CORM A1 treated group at the transcript level (Fig 3.8b) but protein expression did show lowered *P53*

(Fig 3.8c). Though non-significant changes were observed in transcript of *P53* in ox-LDL treated HUVEC and MDMs, CORM A1 treatment had accounted for a decrement in *P53* transcripts. Further, levels of *NF-kb* showed significant elevation in pro-atherogenic milieu in thoracic aorta of SD rats as well as ox-LDL treated HUVECs and MDMs. A significantly reduced expression of *NF-kb* was observed in CORM-A1 treated groups (Fig 3.8b). Cumulatively, CORM-A1 represses expression of transcription factors of miR34a-5p in atherogenic conditions.

Zeb1, *Snai1* and *Stat3* are known transcriptional inhibitors of miR34a-5p. On assessing their status, we found decreased expression in the thoracic aortae of ath diet fed SD rats whereas the same were upregulated in the aortae of CORM-A1 treated group (Fig 3.9c). *Zeb1* and *Stat3* titers were elevated in ox-LDL treated HUVEC, with non-significant changes in *Snai1* (Fig 3.9a). Whereas atherogenic MDMs showed significant decrement in *Snai1* and *Stat3* levels (Fig 3.9b). CORM-A1 treatment accounted for significant elevation in expression of all the transcriptional inhibitors. Overall, atherogenic HUVECs and MDMs plausibly, physiologically attempt to cope up with the stress by elevating expression of different transcription inhibitors expressed in cell specific manner, whereas other inhibitors are being downregulated. CORM-A1 treatment significantly upregulates the expression of all the transcription inhibitors culminating in lowered expression of miR34a-5p.

CORM-A1 alleviates miR34a-5p by epigenetic regulation on its promoter region

CpG islands undergo aberrant methylation in several pathological conditions including CVDs. To determine potential mechanism of miR34a-5p elevation and subsequent alleviation by CORM-A1 we analyzed the promoter region that had CpG island about

300 bp upstream of transcription start site. MSP assay revealed hypomethylation in atherogenic HUVEC and MDMs represented as significantly lowered methylation and increased unmethylation in ox-LDL treated cells that basically facilitates higher transcription rate and subsequent elevation of miR34a-5p. The same was reverted in CORM-A1 co-supplemented group (Fig 3.10a & b). The results showed that CORM-A1 re-methylates the CpG island in promoter region facilitating lowered rate of transcription and thus miR34a-5p expression.

Assessing physical interaction of CO with the transcription factors P53 and NF-κB

CORM-A1 on introduction into the biological system releases CO in slow and controlled manner. CORM-A1 mediated lowering of transcription factors was assessed by gene expression analysis. Herein we further try to assess any physical interaction of CO moiety to the any domain of P53 and NF-κB as a part of plausible regulatory method using computational program (Fig 3.11 a-d). Wherein the Glide g Score of CO in a best pose was -1.131 kcal/ mol. The ligand interaction analysis demonstrated a conventional hydrogen bond of CO with the residue VAL 61 of NF-κB.

Another Docking interaction of CO with p53 was analysed. The Glide g Score of CO in a best pose was -3.039 kcal/ mol. The ligand interaction analysis demonstrated conventional hydrogen bond of CO with the amino acid residue LYS 132 of NF-κB. Another C-H bond with ARG 273 was observed along with attractive charges of CO for residues LYS 132 and GLU 271 of p53 (Table 3.1). It was evident from the Glide score and protein-ligand interaction analysis that CO showed higher affinity and stronger binding towards the target p53.

Prime energy of Protein ligand complexes was also calculated by the prime suite. It revealed the relative binding values ligand CO with targets NF-κB and p53 as -11989.4 and -6917.0 respectively. Binding free energy distributions of ligand CO with the targets NF-κB and p53 were observed and enumerated as shown in the table. On the basis of free energy values, CO showed higher selectivity towards the target p53 compared to NF-κB. Free energy calculations here helped in providing insights into the selectivity of ligand with targets NF-κB and p53 (Table 3.2). However, for a better understanding selective docking analysis of CO in the DNA binding domain of the said proteins (Fig 3.11 e & f) can further reveal CO mediated impending interaction of transcription factors and the transcription start site of the miRNA resulting into lowered miR34a-5p production.

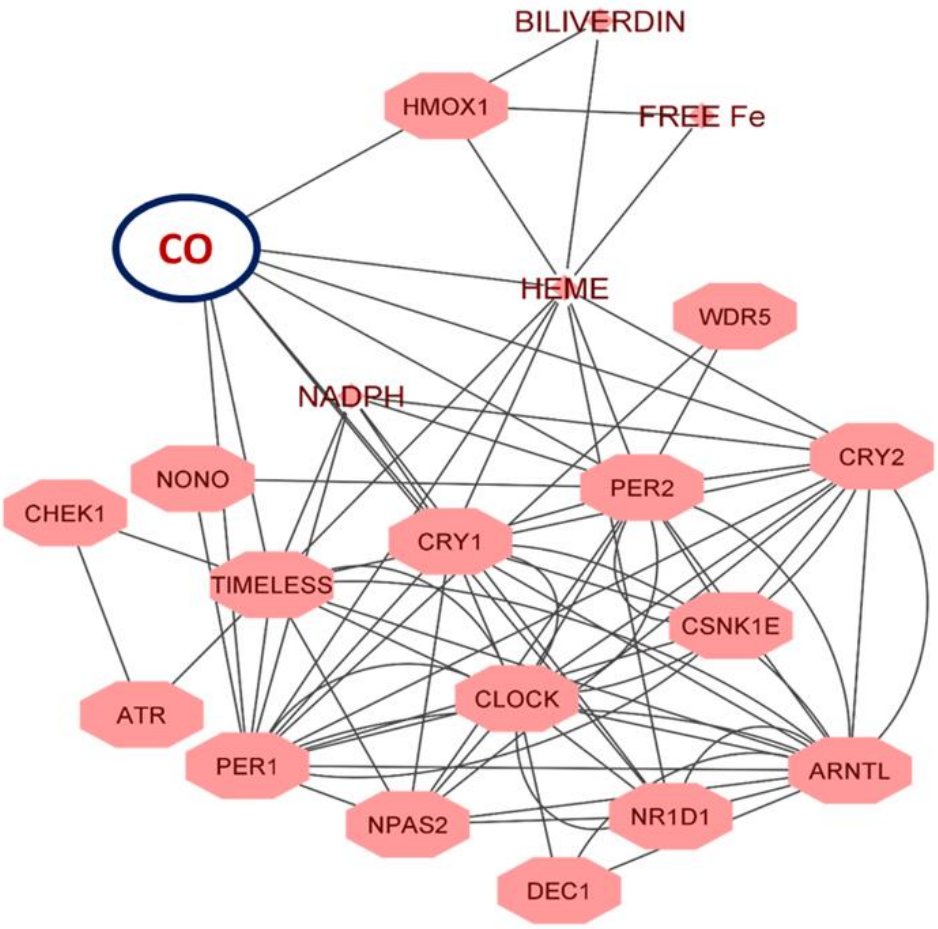

Fig. 3.1: Network diagram of carbon monoxide (CO) association and regulation of circadian clock genes.

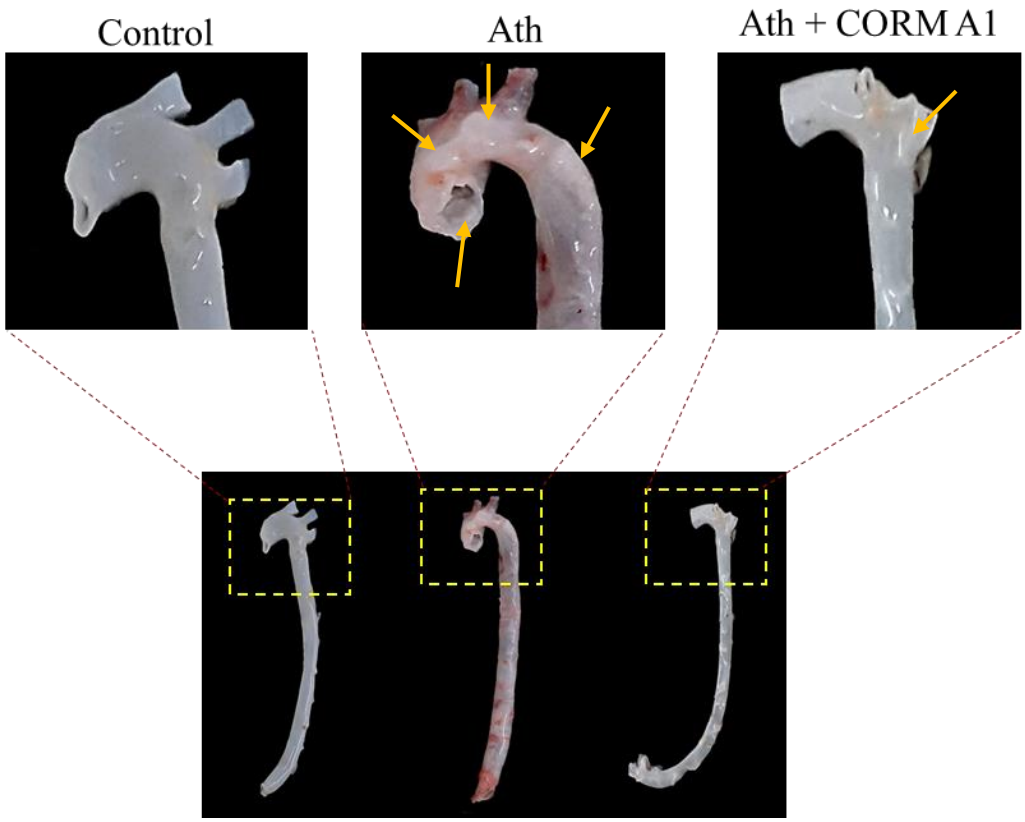

Fig. 3.2: Sprague Dawley rats were fed of atherogenic diet only/or treated with CORM-A1 (2mg/Kg). *En face assay* was done by isolating and cleaning the thoracic aortae from all the animals. Images were taken using Nikon D5300 camera and digitally magnified for clear visualization of atherogenic lesion development, marked with yellow arrows.

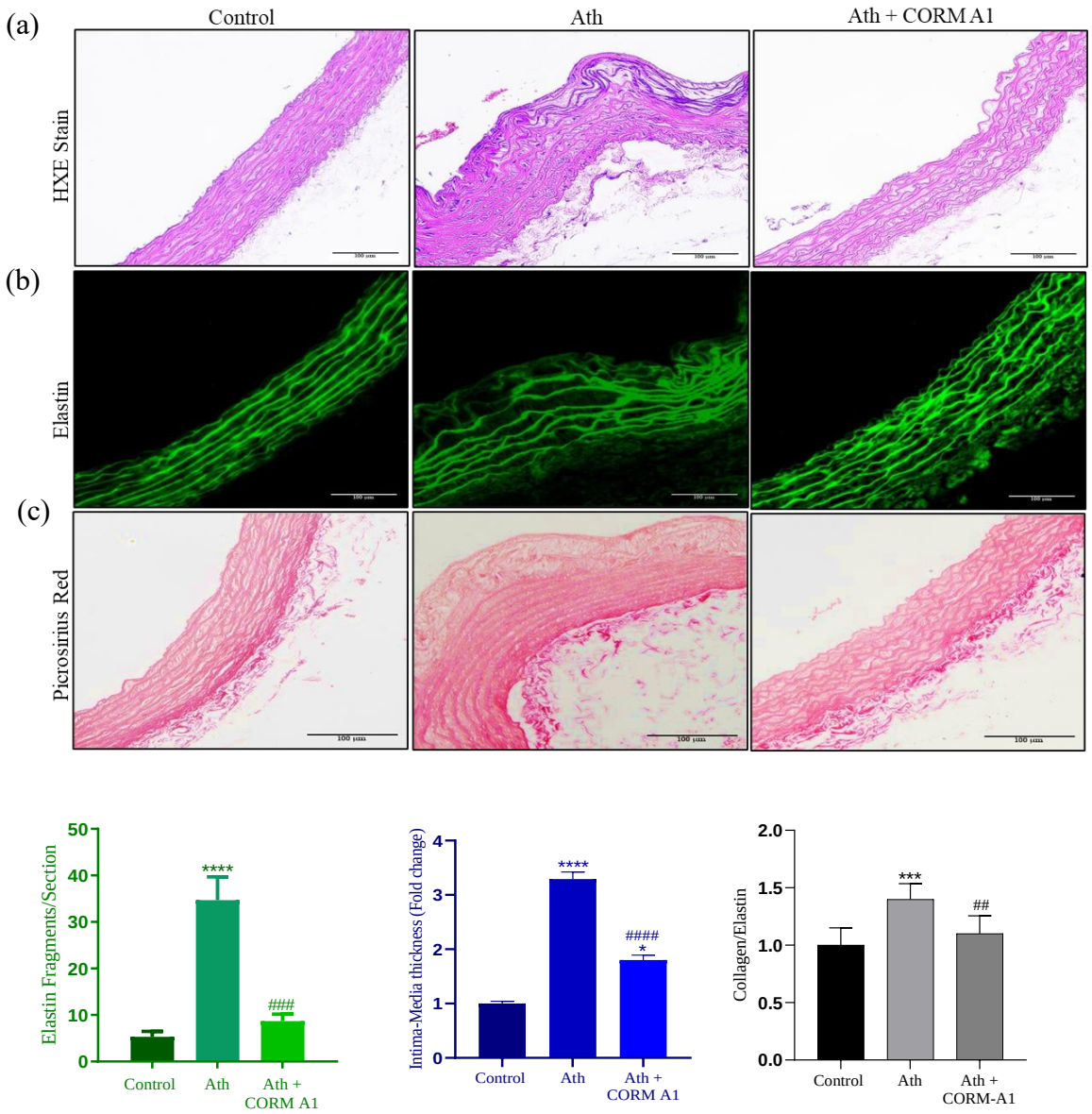

Fig. 3.3.1: Thoracic aortae of Sprague Dawley rats fed on atherogenic diet and/or CORM-A1 were evaluated for pro-atherogenic changes. The histoarchitecture was assessed by (a) H&E staining revealed altered intima-media thickening, represented graphically as fold change. Vascular fibrillar analysis was done by (b) assessing elastin derangement and fragmentation represented graphically as fragmentations/section. (c) Collagen content and organization was estimated by Picrosirius Red staining (Scale 100µm). arterial stiffening and vasomotor tone were estimated by collagen to elastin ratio represented graphically. Results are expressed as mean ± S.E.M. *p < 0.05, **p < 0.01, ***p < 0.001 or ****p < 0.0001 is when compared to control group and #p < 0.05, ##p < 0.01, ###p < 0.001 or ####p < 0.0001 when compared to atherogenic (disease) group.

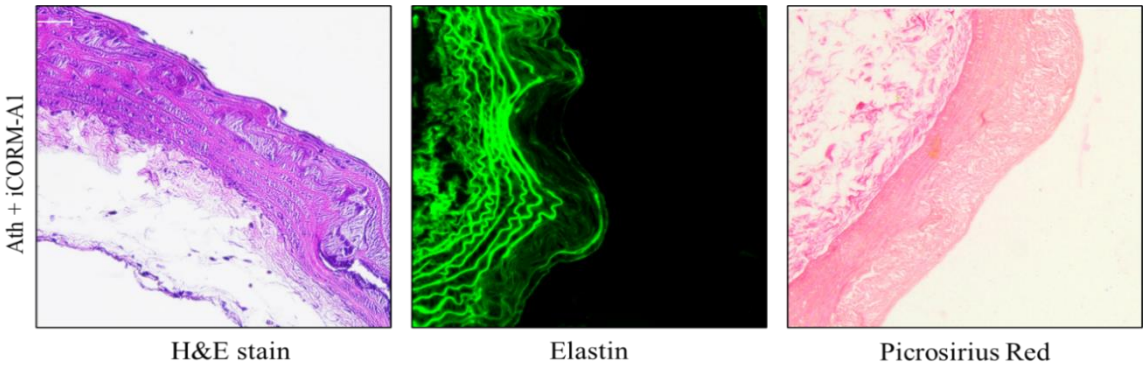

Fig. 3.3.2: Thoracic aortae of Sprague Dawley rats fed on atherogenic diet and iCORM-A1 (inactive CORM-A1) were evaluated for pro-atherogenic changes in terms of H&E staining, Elastin derangement and fragmentation and Picrosirius Red staining.

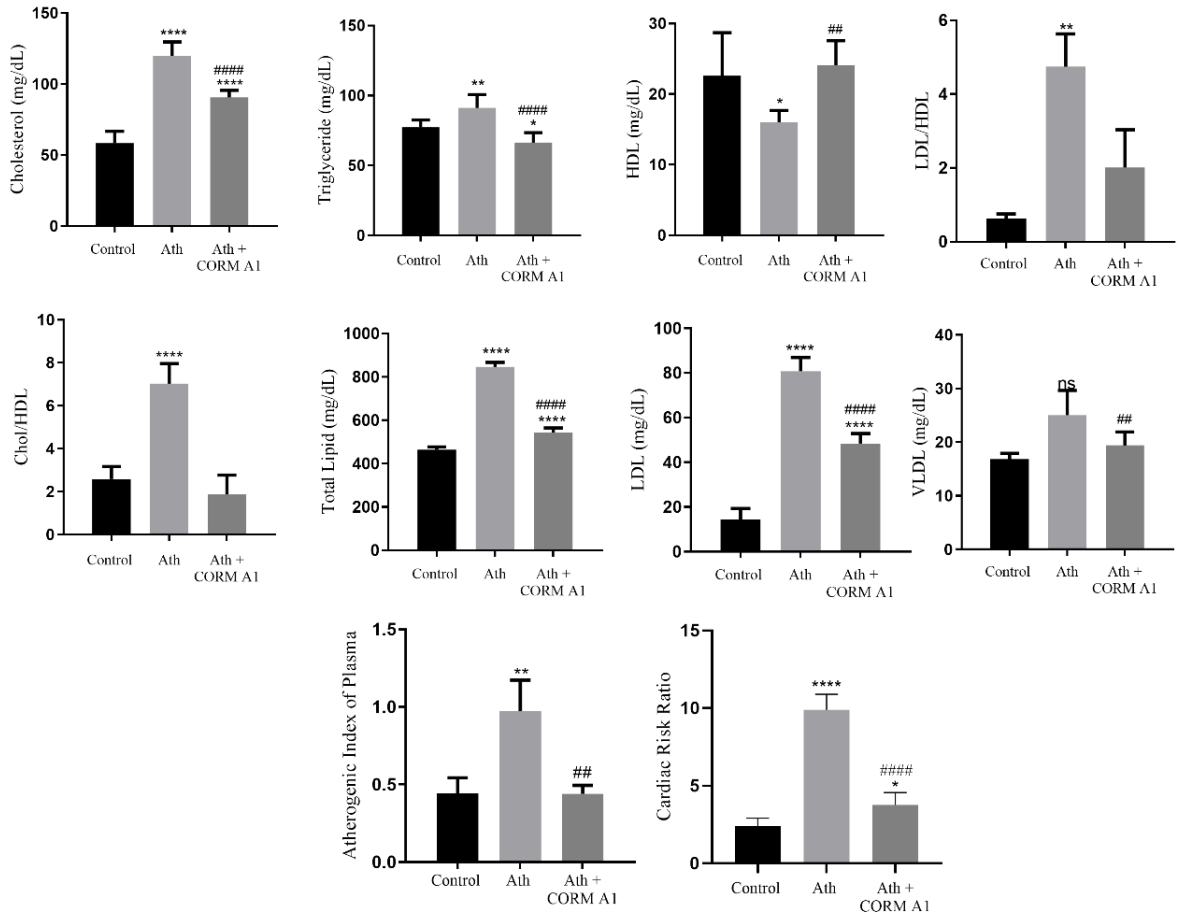

Fig. 3.4: Whole blood collected from Sprague Dawley rats was used for studying (a) complete serum lipid profile including total cholesterol (TC), Triglyceride (TG), HDL, LDL, Total lipid and VLDL measured in mg/dL. (b) Atherogenic Index of Plasma (AIP) and Cardiac Risk Ratio (CRR) were calculated (formula mentioned in Material and Methods chapter) as per the formulae revealing atherogenic conditions (n=5). Results are expressed as mean ± S.E.M. *$p < 0.05$, **$p < 0.01$, ***$p < 0.001$ or ****p < 0.0001 is when compared to control group and $^{\#}p < 0.05$, $^{\#\#}p < 0.01$, $^{\#\#\#}p < 0.001$ or $^{\#\#\#\#}$p < 0.0001 when compared to atherogenic (disease) group.

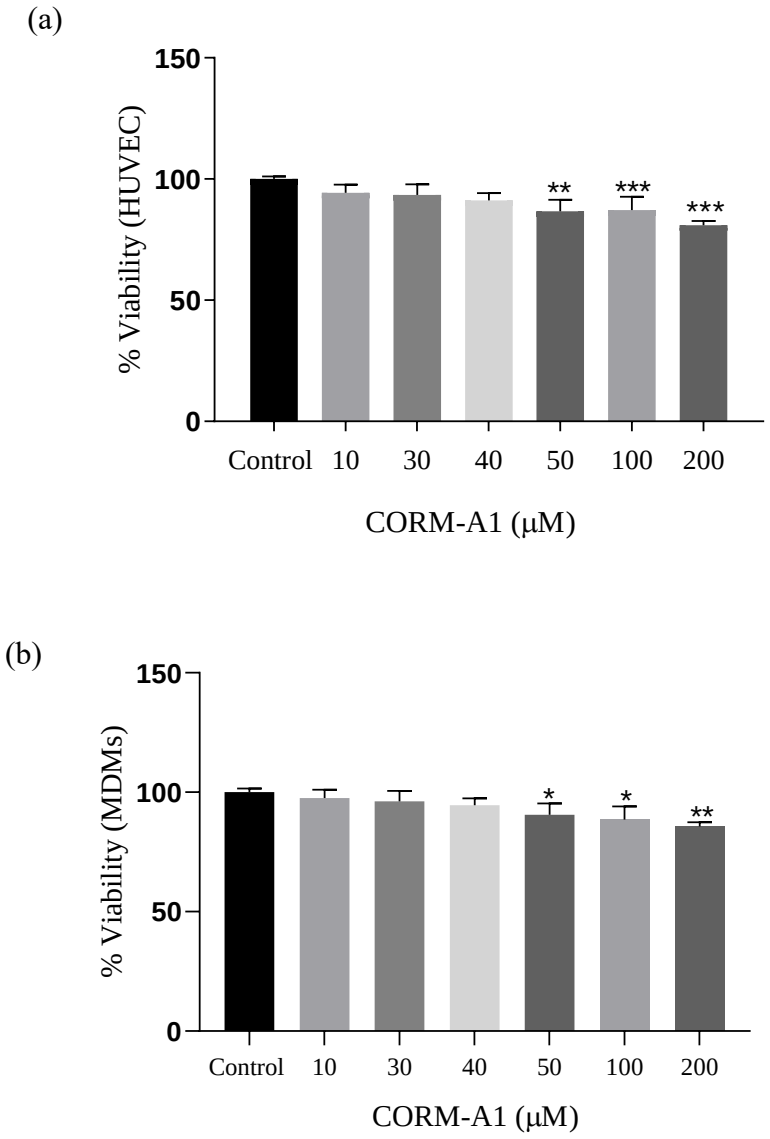

Fig. 3.5: Cytotoxicity of CORM-A1 evaluated at different doses (10, 30, 40, 50, 100 and 200 μM) on HUVEC (a) and MDMs (b) using MTT assay. Represented graphically as % viability. Results are expressed as mean ± S.E.M. *$p < 0.05$, **$p < 0.01$, ***$p <$ 0.001 or ****p < 0.0001 is when all the groups are compared to control group.

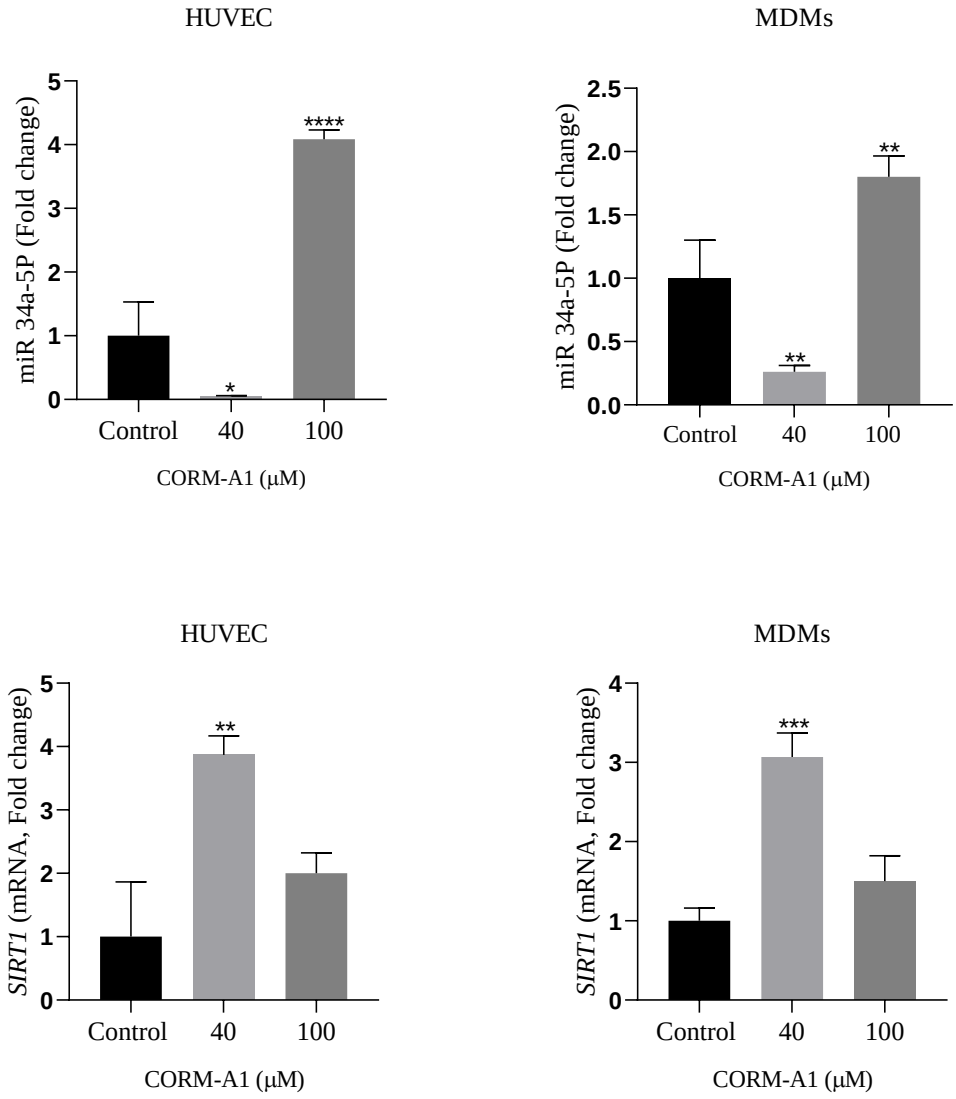

Fig. 3.6: physiological assessment of CORM-A1 on expression of miR34a-5p and its gene target SIRT1 was done at 40 and 100 μM doses. miRNA and mRNA are expressed as fold change and normalized with 5S and 18s rRNA respectively (n=3). Results are expressed as mean ± S.E.M. *$p < 0.05$, **$p < 0.01$, ***$p < 0.001$ or ****$p < 0.0001$ is when compared to control group.

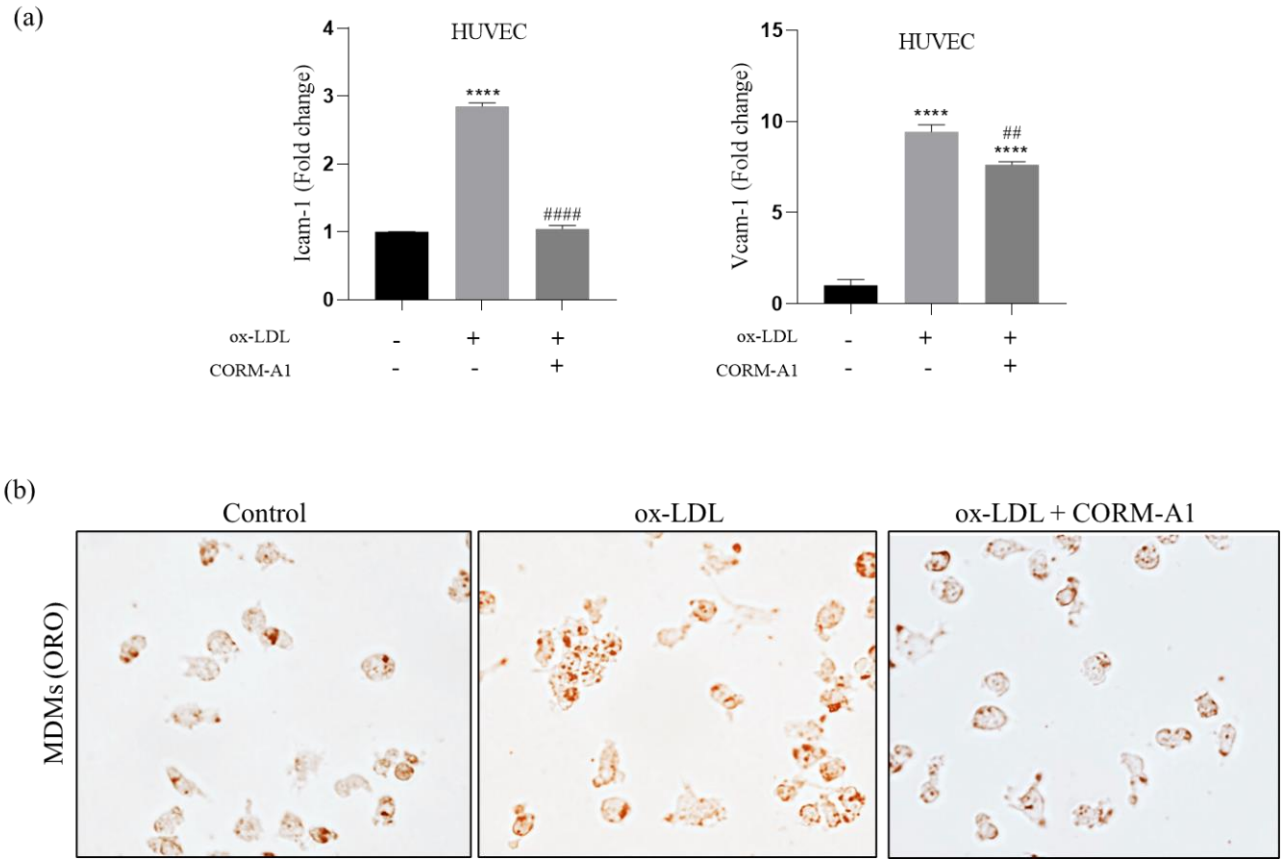

Fig. 3.7: Atherogenic model development in HUVEC and MDM was assessed as endothelial cell activation and expression of adhesion molecules (a) *ICAM-1* and *VACM-1* quantified by qPCR analysis for HUVECs (n=3). Foam cell formation was assessed with lipid retention determined with ORO staining in MDMs. Cell imaging was done using Leica inverted bright field microscope. Results are expressed as mean ± S.E.M. *$p < 0.05$, **$p < 0.01$, ***$p < 0.001$ or ****$p < 0.0001$ is when compared to control group and $^{\#}p < 0.05$, $^{\#\#}p < 0.01$, $^{\#\#\#}p < 0.001$ or $^{\#\#\#\#}p < 0.0001$ when compared to atherogenic (disease) group.

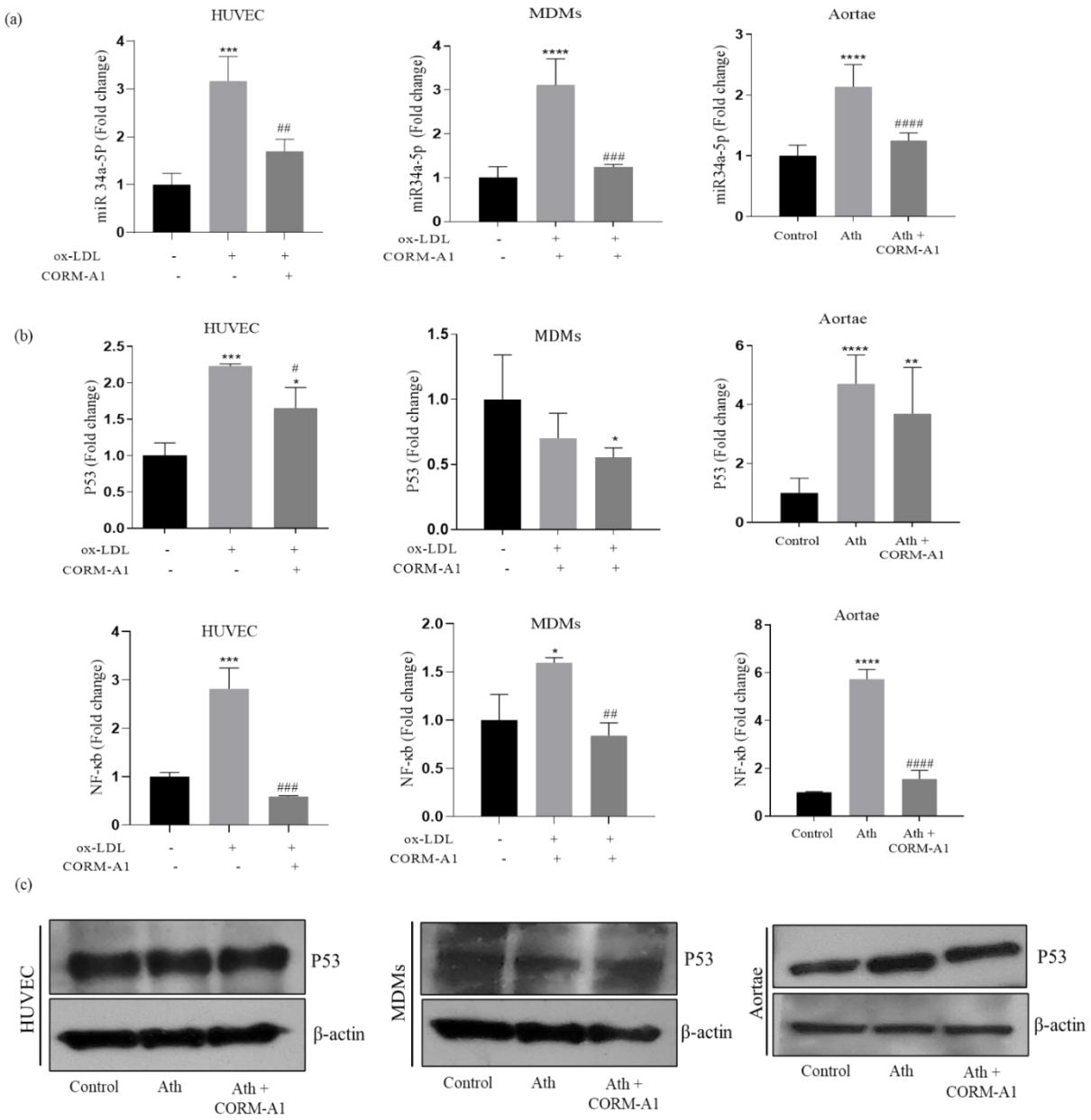

Fig. 3.8: (a) Levels of miR34a-5p were assessed in all the experimental models (HUVEC, MDMs and aortae of SD rats) and normalized with *5S*. (b) Transcription factors of miR34a-5p were assessed by qPCR analysis and normalized with *18s RNA* for cells and *GAPDH* for aortae. (c) Western blot analysis for P53 normalized with housekeeping gene β-actin. Results are expressed as mean ± S.E.M. *$p < 0.05$, **$p < 0.01$, ***$p < 0.001$ or ****$p < 0.0001$ is when compared to control group and $^{\#}p < 0.05$, $^{\#\#}p < 0.01$, $^{\#\#\#}p < 0.001$ or $^{\#\#\#\#}p < 0.0001$ when compared to atherogenic (disease) group.

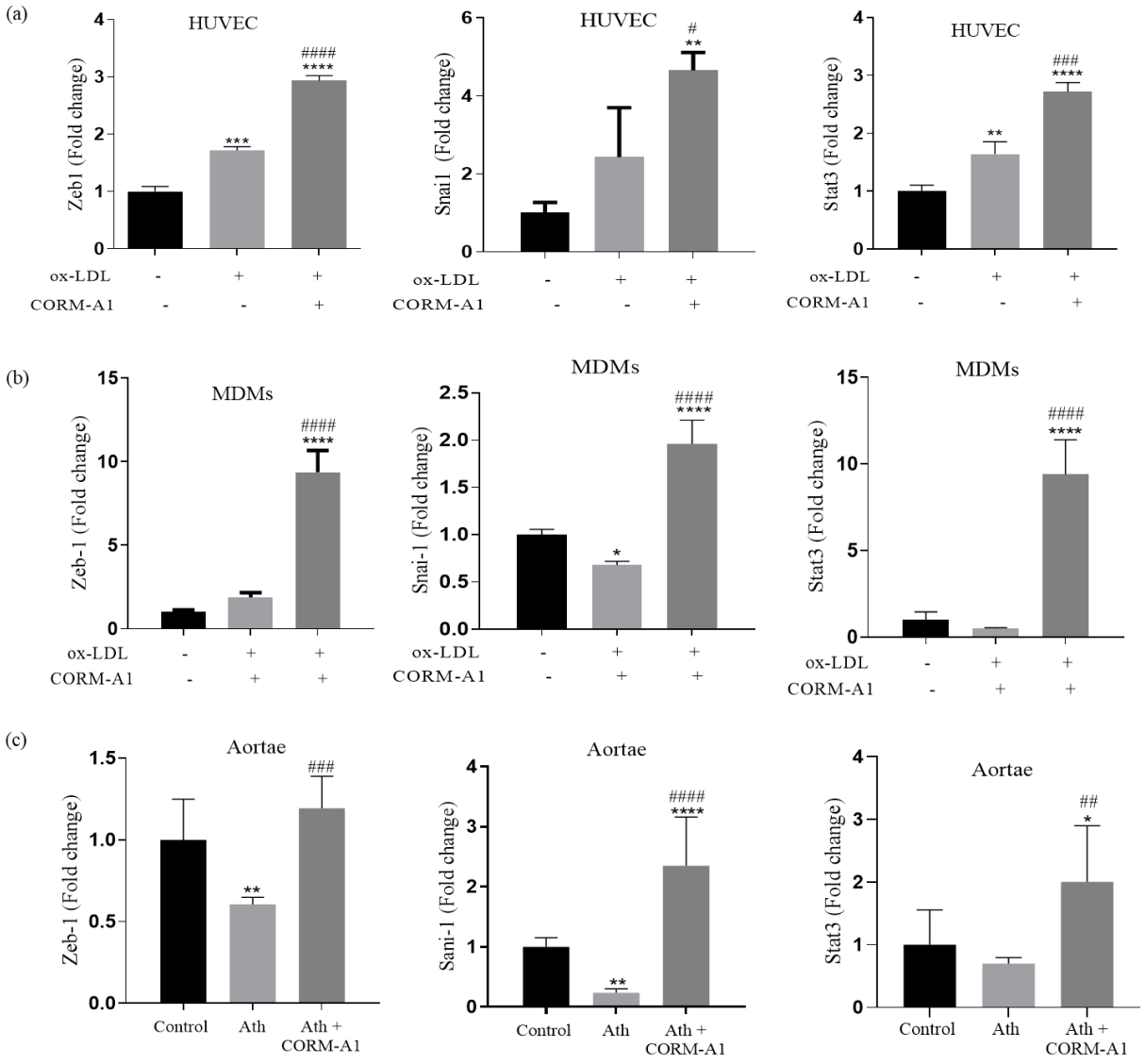

Fig. 3.9: miR34a-5p transcription inhibitors *Zeb-1, Snai1* and *Stat3* were quantified in (a) HUVEC, (b) MDMs and (c) thoracic aortae by qPCR and normalized with *18s rRNA* and *GAPDH*, respectively. Results are expressed as mean ± S.E.M. *$p < 0.05$, **$p < 0.01$, ***$p < 0.001$ or ****$p < 0.0001$ is when compared to control group and $^{\#}p < 0.05$, $^{\#\#}p < 0.01$, $^{\#\#\#}p < 0.001$ or $^{\#\#\#\#}p < 0.0001$ when compared to atherogenic (disease) group.

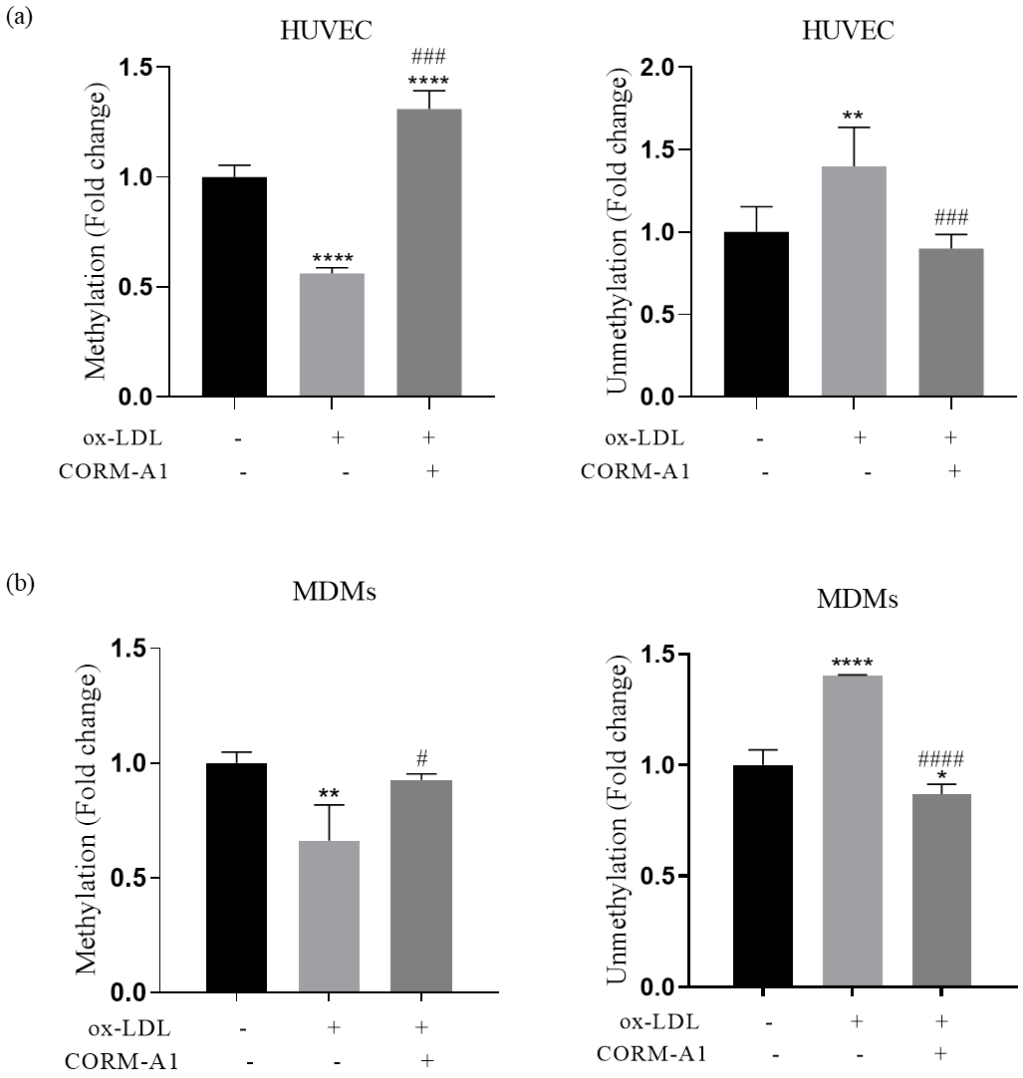

Fig. 3.10: Epigenetic modification in disease condition and CORM-A1 treated (a) HUVEC and (b) MDMs were assessed in cells by MSP assay. Methylation pattern alterations were seen in the CpG island found about 300 bp upstream of the transcription start site. Primers were designed to assess methylation and unmethylation in the region. Results are expressed as mean ± S.E.M. *$p < 0.05$, **$p < 0.01$, ***$p < 0.001$ or ****$p < 0.0001$ is when compared to control group and $^{\#}p < 0.05$, $^{\#\#}p < 0.01$, $^{\#\#\#}p < 0.001$ or $^{\#\#\#\#}p < 0.0001$ when compared to atherogenic (disease) group.

(a)

(b)

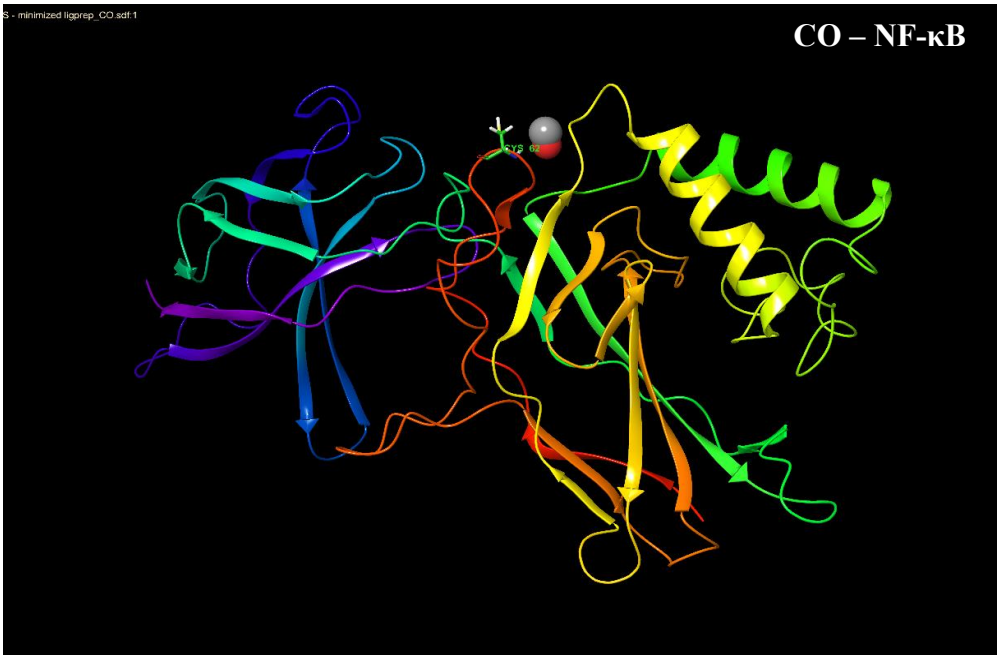

(c)

CO – P53

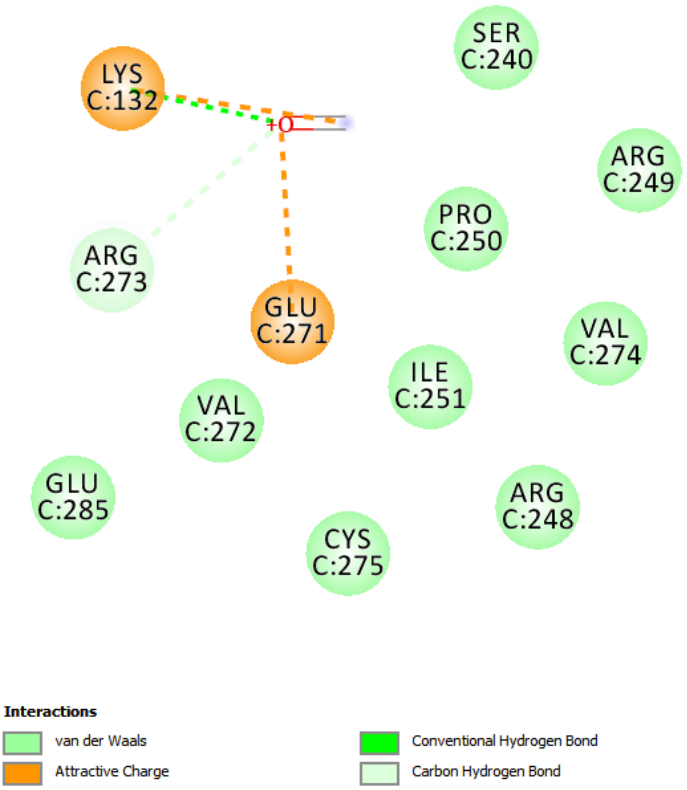

(d)

CO – NF-κB

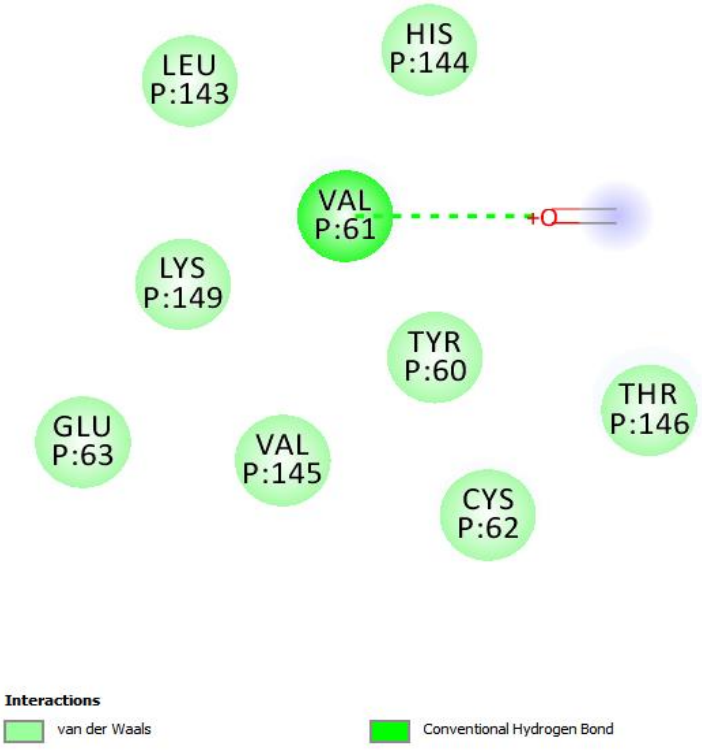

(e)

DNA – P53

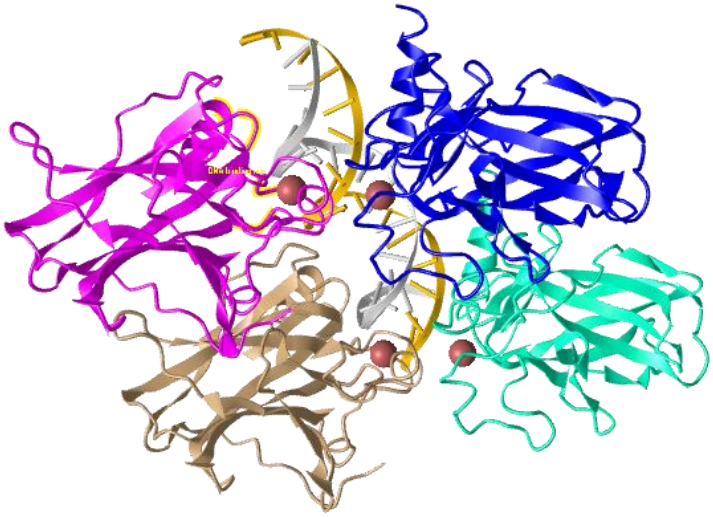

(f)

DNA – NF-κB

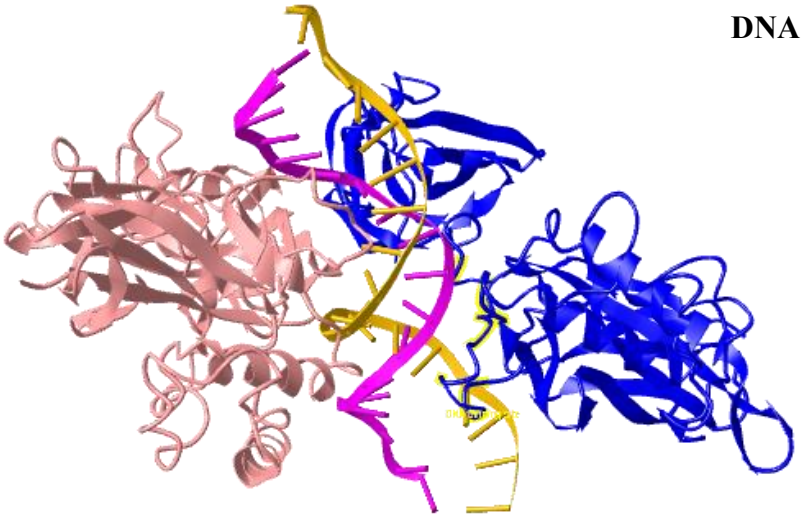

Fig. 3.11: Association of carbon monoxide molecule with miR34a-5p transcription factors P53 and NF-κB was assessed for docking that is represented as (a) molecular docking pose of CO with P53 and NF-κB respectively. (b) 2D interaction map of CO and protein interaction. (c) DNA binding domain of these proteins were identified and represented in ribbon structure. The yellow part of the protein represents interaction with DNA.

Protein Name	Glide Score (kcal/mol)	H-bond Interactions
NF-kb	-1.131	Val 61
P53	-3.039	Lys 132

Table 3.1: Docking score and interactions of CO with target proteins NF-κB and P53.

Target Name	Bind Energy (kcal/mol)	Bind coulomb	Bind (NS) (kcal/mol)	Bind (NS)-Coulomb	Prime MM-GBSA ligand efficiency	Prime energy of PL complex
NF-κB	-6.781	0.038	-6.781	0.038	-5.085	-11989.4
P53	-8.289	-0.645	-8.289	-0.654	-6.217	-6917.0

Table 3.2: Free energy calculations (MM-GBSA) of CO bound to NF-kb and p53.

Discussion

In recent years miRNAs have come to light for their vital physiological and pathological implications. In previous chapters miR34a-5p has been demonstrated as a circadian clock associated miRNA. miR34a-5p regulated CLOCK gene expression by binding to its 3'UTR as assessed in HUVECs and also observed in thoracic aortae of C57BL/6J mice. The thoracic aorta of chronodisruptive C57BL/6J mice, harbouring elevated miR34a-5p titers, showed pro-atherogenic manifestations. That was in agreement to several published literature that showed presence of elevated miR34a in atheromatous plaque of the CVD patients. Thus, a detailed investigation was designed with atherogenic model developed in SD rats by feeding them atherogenic diet.

CO is an endogenous gasotransmitter produced on heme degradation, a reaction facilitated by enzyme called HO-1 with equal ratio of bilirubin as by-product of the reaction. CO has been studied for its varied functions that on one hand encompasses circadian functioning and on other is reported for its vasomotor regulation properties. A study conducted in patients with CVD showed elevated titers of CO as compared to the control patients. In our model system, if an indirect approximation was made, a similar trend was observed in titers of bilirubin that were elevated in SD rats fed with ath diet. Alongside, miR34a-5p also exhibited its functional implications in two similar physiological processes of chronobiology and vascular physiology as CO. With an understanding of elevated CO as a biological coping mechanism and elevated miR34a-5p in vascular pathology, we decided to test impact of CO on miR34a-5p expression.

The experimental in-vivo model developed in SD rats was fed ath diet in an attempt to closely associate physiological alterations with that of high calorie diet intake relating to current lifestyle of the people. CORM-A1 was administered exogenously to the rat

as miR34a-5p modulator. Atherogenic disease model validation was done with H&E staining wherein the aortae showed intimal-media thickening along with elastin fragmentation. The vasomotor tone assessed with collagen to elastin ratio revealed arterial stiffening, observation in agreement to the result of *en face* assay. Further all these changes were reversed towards normalcy in CORM-A1 treated animals. In-vitro experimentations with HUVECs and MDMs treated with CORM-A1 (40 μM) had shown reduction in miR34a-5p titers in normal physiological conditions. Establishing the correlation, CORM-A1 was further assessed for its miR34a-5p mediated alleviation of pro-atherogenic changes. Ox-LDL (80μg/mL) dosed to HUVEC and THP-1 derived MDMs for developing invitro atherogenic models. The same was validated by assessing expression of adhesion molecules marking endothelial cell activation and ORO staining marking foam cell formation in the respective cells. Co-supplementation with CORM-A1 had shown anti-atherogenic effect by reverting the expression in the culture systems as well.

Further it was aimed to assess the transcription control of miR34a-5p that falls in the category of intergenic miRNA, meaning it has its own promotor region and is transcribed independent to that of the host gene. miR34a-5p has been extensively studied with P53 as its transcription factor, majorly in cancers. miR34a – P53 have been shown to have tight feedback loop system regulating their expression. Studies have also reported inflammatory gene NF-κB as other transcription factor of miR34a (Li *et al.*, 2012). Herein we found elevation in titers of both the transcription factors in atherogenic model. CORM-A1 treatment had accounted for reduction in production of transcription factors. Further Zeb1, Snai1 and Stat3 were assessed as transcription inhibitors of miR34a-5p (Slabáková *et al.*, 2017; Shi *et al.*, 2019). Interestingly, these genes were differentially expressed in cell specific manner. However, CORM-A1

treatment had elevated expression of Zeb1, Snai1 and Stat3 in all the three disease models.

Aberrant DNA methylation is a physiological response to stout external stimuli (Tost, 2010). Altered circadian rhythms have been shown to manifest DNA methylation in biological systems and manipulate gene expression (Azzi *et al.*, 2014). Moreover, pathological conditions like cancer, CVDs, etc. have also been reported for aberrant DNA methylation. Thus, herein we aimed to assess the plausible alterations in DNA methylation patterns in promoter region of miR34a-5p about 300bp upstream of the transcription start site. The atherogenic cells had shown elevating unmethylation in the promoter region and complementing lowered methylation implying to facilitated increase in rate of miRNA transcription. Cells co-treated with CORM-A1 showed opposing resulting to that of the disease conditions. The methylation pattern was almost reverted back, comparable to the control.

Apart from direct biological implication at gene and protein level we also attempted to understand if CO physically associated with any of the transcription factor to impend the miR34a-5p transcription. The data obtained for molecular docking, relative free binding energies, from MMGBSA analysis showed CO binding relatively strongly to P53 as compared to NF-κB. It would be rather interesting to further assess if CO docking was inside any of the DNA binding domain of these proteins.

Overall, this study is a compile of developing atherogenic model in SD rats, HUVEC and MDMs to evaluate miR34a-5p expression in the said pathology and decipher its mechanism. The study also talks about miRNA modulator CORM-A1 that has shown its anti-atherogenic properties, believed to be orchestrated by lowering of miR34a-5p in the disease conditions.